Published in final edited form as:
J Biophotonics. 2013 August ; 6(8): 567–572. doi:10.1002/jbio.201200110.

Raman spectroscopy provides a powerful, rapid diagnostic tool for the detection of tuberculous meningitis in *ex vivo* cerebrospinal fluid samples

R. Sathyavathi[1], **Narahara Chari Dingari**[2], **Ishan Barman**[2], **P. S. R. Prasad**[3], **Subhashini Prabhakar**[4], **D. Narayana Rao**[1], **Ramachandra R. Dasari**[2], and **Jayanthi Undamatla**[5,6,*]

[1]School of Physics, University of Hyderabad, Hyderabad, India

[2]George R. Harrison Spectroscopy Laboratory, Massachusetts Institute of Technology, Cambridge, USA

[3]National Geophysical Research Institute (Council for Scientific and Industrial Research), Hyderabad, India

[4]Apollo Hospitals, Hyderabad, India

[5]Apollo Hospitals Education & Research Foundation, Hyderabad, India

Abstract

In this letter, we propose a novel method for diagnosis of tuberculous meningitis using Raman spectroscopy. The silicate Raman signature obtained from *Mycobacterium tuberculosis* positive cases enables specific and sensitive detection of tuberculous meningitis from acquired cerebrospinal fluid samples. The association of silicates with the tuberculosis mycobacterium is discussed. We envision that this new method will facilitate rapid diagnosis of tuberculous meningitis without application of exogenous reagents or dyes and can be aptly used as a complementary screening tool to the existing gold standard methods.

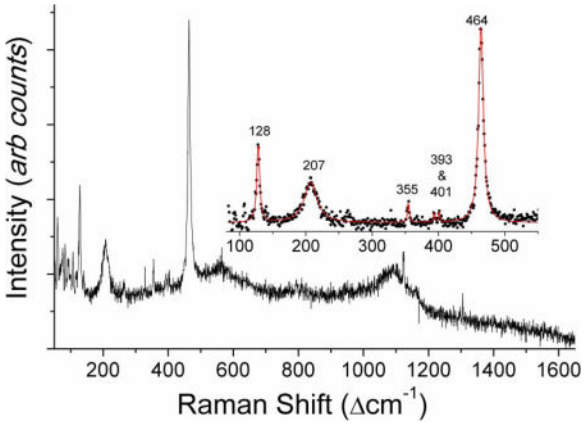

*Corresponding author: jayanthiundamatla@gmail.com, Phone: +91-40-23357048, Fax: +91-40-2335 7046.
[6]Sandor Proteomics Pvt. Ltd., Hyderabad, India (current address)

Typical Raman spectra of the CSF sample clinically diagnosed as tuberculosis meningitis.

Keywords

tuberculous meningitis (TBM); cerebrospinal fluid (CSF); Raman spectroscopy; silicates

1. Introduction

Tuberculosis (TB) remains one of the major causes of death from a single infectious agent (*Mycobacterium tuberculosis*) across the world. Over 8.3 million new cases and 2 million deaths occur annually in developing countries [1]. In India alone, 2.2 million people are affected annually and about 400,000 people die due to tuberculosis [2]. Tuberculosis is known to appear both in pulmonary and extra pulmonary forms. In particular, extra pulmonary tuberculosis involves relatively inaccessible sites and, because of the nature of the sites involved, fewer bacilli can cause much greater damage. The combination of small numbers of bacilli and inaccessible sites causes bacteriologic confirmation of a diagnosis to be more difficult, and invasive procedures are frequently required to establish a diagnosis.

Tuberculous meningitis (TBM) is an infection of the meninges, and form of extra pulmonary tuberculosis regarded as a medical emergency [3]. Meningitis can result from direct meningeal seeding and proliferation during *M. tuberculosis* bacillemia either at the time of initial infection or at the time of breakdown of an old pulmonary focus. It can also result from the breakdown of an old parameningeal focus with rupture into the subarachnoid space. The consequences of subarachnoid space contamination can be diffuse meningitis or localized arteritis. In TBM, the process is located primarily at the base of the brain [4]. Ominously, in untreated TBM, the mortality rate is almost 100% and delay in treatment may lead to permanent neurological damage [3]. Consequently, early diagnosis and prompt treatment are the primary factors determining the final outcome of the patient.

Unfortunately, at present, the diagnosis of TBM remains a challenge due to its pleomorphic clinical presentations and the lack of a rapid sensitive and specific test. Typically, the clinical sample that is employed in TBM diagnosis is cerebrospinal fluid (CSF) collected by lumbar puncture. For diagnosis of TBM, mycobacteria identification is necessary. This is done by either acid fast staining of the bacilli (AFB), conventional Lowenstein Jensen (LJ) microbiologic culture or molecular assays such as polymerase chain reaction (PCR). All these techniques have limitations for detection due to low copy number or slow growth rate of the bacilli, which causes delays in obtaining results and consequently leads to permanent neurological disorders and high mortality rates [3, 4].

In view of these limitations, there is a need for a fast, simple alternative diagnostic assay that can be readily applied to CSF for the diagnosis of TBM. In this regard, spectroscopic detection offers the capability for direct analysis of cellular structures in microbial bulk samples [5, 6] or body fluids [7, 8] since it provides detailed molecular information of the investigated samples. In particular, Raman spectroscopy provides a valuable non-perturbative probe that can enable fingerprinting of analytes (based on their vibrational signatures) in biological samples in a few seconds without necessitating the addition of

staining or other chemical reagents [9, 10]. Indeed, several investigators have shown that Raman spectroscopy (and specific embodiments of the same) can generate a wealth of information and facilitate trace analyte detection even in complex matrices such as whole blood samples and biological tissue [11–13]. The promising results of Raman studies [14–17] for *in vitro* diagnosis prompted us to investigate CSF samples of suspected TBM cases for their corresponding Raman signatures. The TBM studies reported here demonstrate the acquisition of Raman spectra in the CSF matrix of multiple clinical samples and show an initial attempt at developing a classification algorithm to discriminate prospective spectra obtained from unknown clinical samples. Our results underline the clinical potential of Raman spectroscopy as a biomedical assay for rapid TBM screening in CSF of suspected patients.

2. Experimental

2.1 Materials and methods

2.1.1 Patient population and CSF preparation—This *ex vivo* study was conducted at Apollo Hospitals, Hyderabad and approved by local ethics committee, under a waiver of informed consent, as the CSF samples were considered discarded samples (bio-waste). CSF samples from a total of 60 patients (25 female patients with mean age of 48.4 years and 35 male patients with mean age of 53.6 years) were employed in this study. Eleven patients were clinically diagnosed as TBM positive at the time of the study. In addition, three patients had culture-proven non-TBM, four patients had viral meningitis, and 42 patients had other non-infectious disorders. No patient was on anti-tubercular therapy at the time of the CSF sample collection. For Raman measurements, the samples were cytospinned on microscopic glass slides and allowed to air dry at room temperature, before being fixed with isopropyl alcohol then stored at room temperature until used.

2.2 Raman experiments

Raman spectra were collected using a micro-Raman spectroscopy unit (at the National Geophysical Research Institute, Hyderabad), consisting of a Jobin Yvon confocal microanalysis system (JY T-64000) attached to an Olympus microscope (model U-LH 100/3). The excitation source was a 514.5 nm air cooled argon ion laser (Spectra Physics). Typically, 3 mW of excitation light was focused on the sample and the Raman scattered light was collected in a backscattering geometry through the microscope objective (50X, NA 0.7). The Raman scattered light was dispersed through the triple monochromator system operating in subtractive mode onto a liquid nitrogen cooled CCD detector (Symphony, JY Inc.). The spectral resolution of the system was *ca.* 2 cm^{-1} and the reproducibility of the Raman peaks' position was within 1 cm^{-1}.

The acquisition time for all Raman spectra was 30 seconds. More than 5 replicate spectra were recorded using different spatial locations on each of these cytospin preparations. Wavenumber calibration was performed by using the characteristic silicon reference peak at 521 cm^{-1}. The Raman spectra were subjected to standard baseline removal and peak fitting procedures using the GRAMS/3 software. The relevant clinical information (class label and

spectral dataset) with donor information removed was submitted to the MIT Spectroscopy Laboratory for analysis and interpretation of the spectroscopic results.

3. Results and discussion

The purpose of this study is not only to enable classifier development but also to assess the clinical relevance of the same with respect to manifestations of TBM in CSF. To this end, as pointed out by Somorjai and co-workers, classifiers or classifier combinations lacking selection of specific features are of limited value when applied to the acquired Raman spectra [18]. This is because even though diagnosis and (potentially) prognosis is of substantive importance, they form only a portion of the entire clinical story. Here, as a proof-of-concept study, the larger importance lies in the identification of a few, biologically relevant discriminatory features (i.e. specific Raman signatures, or peaks) that could lead to an effective understanding of the disease mechanism that could in turn assist in the management and treatment of such a disorder. To this end, we perform classification of the samples using ratios of the critical peaks as described below, instead of full spectral analysis.

Figure 1(a) shows a typical Raman spectrum from a CSF sample which was clinically diagnosed as TBM positive. Its corresponding microscopic image is shown in Figure 1(b). From Figure 1(a), we observe the presence of dominant Raman bands at 128, 207, 355, 393, 401 and 464 cm^{-1} due to silicates (quartz α-phase) and a broad peak at 1124 cm^{-1} which can be tentatively attributed to the presence of carbonate compounds. CSF samples demonstrating these silicate and carbonate bands contained crystalline structures (non-specific to the type of chemical present) evident from the microscopic image in Figure 1(b). The strong Raman signature of the silicates was also reproducible as indicated by the near-perfect superimposition of replicate Raman spectra acquired from different locations on the same CSF sample.

In sharp contrast, Figure 2(a) shows a typical Raman spectrum from a CSF sample with clinically diagnosed non-TB meningitis and Figure 2(b) its microscopic image, which lacks the crystalline structures seen in the TBM CSF sample in Figure 1(a). The inset in Figure 2(a) shows the spectrum acquired from a second non-TB meningitis CSF sample which displays features of magnesium carbonate. In the insert, one can visualize the prominent Raman bands at 157 cm^{-1}, 282 cm^{-1}, 556 cm^{-1}, 716 cm^{-1}, 1091 cm^{-1} and 1097 cm^{-1} that corresponds to carbonate species and can be here attributed particularly to the magnesium salt and the calcite form. Table 1 lists the Raman peaks observed and their corresponding origins and symmetry modes.

Our findings in this study were largely consistent with those of Bujitels and co-workers [19], who analyzed 63 strains of various mycobacteria using Raman spectroscopy and validated their results against a gold-standard molecular identification test. They were able to show bacterial signatures in these samples and inferred that Raman spectroscopy is an accurate assay for identification of mycobacterium strains in microbiologic cultures. Our work provides a significant extension of their results as they are derived from direct measurements

on clinical CSF samples and do not necessitate the use of tuberculosis cultures, the growth of which is a time-consuming process.

To quantify the clearly discernible trends in spectral features of CSF samples acquired from patients diagnosed with TBM, we performed peak ratio assessment of the silicate bands. Specifically, the intensity ratio of the average value around 464 cm^{-1} to that around 207 cm^{-1} was used to develop our algorithm (the average was considered over 10 neighboring pixel values) and the decision threshold for TBM diagnosis was set at 1.4. The silicate bands were chosen as the TBM samples present the class of interest for our investigations, and the presence of silicate Raman features would appear to provide an unequivocal positive diagnostic evaluation of TBM. In particular, we observed that the ratio exceeded the aforementioned decision boundary in 10 out of the 11 CSF samples that were clinically diagnosed as TBM in our study. In addition, the algorithm correctly discriminated 40 out of the 49 non-TBM CSF samples (while the other 9 were identified as false positive results). In other words, our empirical algorithm based on the Raman silicate signature provides a sensitivity of 91% and a specificity of 82% for diagnosis of TBM.

For the diagnosis of TBM, sensitivity forms the critical figure of merit for any assay under development. This is because the disease to be diagnosed is serious, should not be missed, and is treatable, and false positive results do not have serious adverse consequences for the patient [20]. In particular, this would be true for the development of a screening assay (such as that envisioned for Raman spectroscopy), which would provide an ideal adjunct to an established molecular identification test. In this case, one would like to identify every single patient with the disease for treatment or further clinical evaluation, even at the cost of making a presumptive diagnosis of TBM in some healthy people that is not confirmed on further testing. From the results of the empirical algorithm, it is evident that Raman spectroscopy provides valuable diagnostic information although one would need to boost the sensitivity (and potentially specificity) for clinical translation. It is worth noting that there is usually a trade-off involved in the maximization of sensitivity and specificity. Therefore, any improvement in sensitivity would likely be obtained at the expense of specificity.

Importantly, our results highlight the strong association between TB and presence of silicates. The association of pulmonary silicosis with tuberculosis is well-established and has been reported by several groups over the years [21–32]. It has been demonstrated that silicon induced growth of *M. tuberculosis* in culture, suggesting a positive role of silicon in mycobaterial pathogenicity [29, 30]. However, this study raises the question as to whether the presence of silicates in the CSF of TBM-affected patients stimulates growth of the bacilli resulting in TBM, or the presence of the bacilli in the CSF somehow accelerates silicate formation. Further our results are supported by the study of Ullas et al. [33], in which they suggested a potential role of CSF for diagnostic purposes. In their study, they also analyzed three CSF samples with various clinical histories that are non-TBM and did not reveal any silicates.

Nevertheless, a substantive amount of research still needs to be performed in order to clarify the precise mechanism of the blood brain barrier and its role in selective filtration of silicates, especially in cases of TBM. This issue is one of the focal points of our current

research, which involves large-scale clinical studies of TBM and non-TBM meningitis disorders. In addition, this ongoing work is likely to reveal cases of meningeal disorders that may have been missed in the current proof-of-concept studies. Accordingly, one would anticipate a switch from an empirical algorithm (employed in this article) to a more rigorous multivariate classification framework that might would feature any combination of machine learning schemes (including but not limited to decision trees, k-nearest-neighbour, artificial neural networks and support vector machines) [34, 35]. For the application of these classification methods, it is important to have a significantly larger dataset in order to ensure a minimum (threshold) sample per feature ratio [18].

4. Conclusion

In summary, we have proposed a novel method for diagnosing TBM from clinical CSF samples by employing Raman spectroscopic measurements. The primary advantages of the proposed methodology are a high degree of intrinsic specificity without necessitating substantive sample preparation (or inclusion of external dyes or reagents) and ability to perform direct measurements on the clinical samples without prolonged microbiologic culture. The silicate signature obtained from Raman spectra of CSF cyto-preparations seen in this study may have potential as a surrogate marker in the diagnosis of TBM. It also highlights the strong association of tuberculosis with silicosis and the possible pathogenic effect of silicates on *M. Tuberculosis.*

Acknowledgments

One of the authors, R. Sathyavathi, acknowledges Department of Science and Technology, Women Scientist project (SR/WOS-A/PS-06/2009) for financial support. NCD, IB and RRD were supported by the National Institute of Health National Center for Research Resources (P41-RR02594). We thank Dr. Swarnltha G., pathologist at Apollo Hospitals, Hyderabad, for providing us with the facility for cytospin. The contributions of Dr. Maryann Fitzmaurice are duly noted in the writing of the final manuscript.

References

1. Training module for medical practitioners. Central TB division. Directorate General of health services, Ministry of Health and family welfare; NirmanBhawan, New Delhi, India: NTCP guidelines. http://www.tbcin-dia.org
2. Katti MK. Med Sci Monit. 2004; 10:RA215–29. [PubMed: 15328498]
3. Venkataswamy MM, Rafi W, Nagarathna S, Ravi V, Chandramuki A. Indian J Med Microbiol. 2007; 25:236–240. [PubMed: 17901641]
4. Ibelings MS, Maquelin K, Endtz HP, Bruining HA, Puppels GJ. J Clin Microbiol Infect. 2005; 11:353–358.
5. Maquelin K, Dijkshoorn L, van der Reijden TJ, Puppels GJ. J Microbiol Meth. 2006; 64:126–131.
6. Goodacre R, Timmins EM, Burton R, Kaderbhai N, Woodward AM, Kell DB, Rooney PJ. Microbiology. 1998; 144:1157–1170. [PubMed: 9611790]
7. Harz M, Claus RA, Bockmeyer CL, Baum M, Rosch P, Kentouche K, Deigner HP, Popp J. Biopolymers. 2006; 82:317–324. [PubMed: 16506165]
8. Harz M, Krause M, Bartels T, Cramer K, Rösch P, Popp J. Anal Chem. 2008; 80:1080–1086. [PubMed: 18197696]
9. Dingari NC, Barman I, Singh GP, Kang JW, Dasari Anal RR. Bioanal Chem. 2011; 400:2871–2880.
10. Dingari NC, Horowitz GL, Kang JW, Dasari RR, Barman I. PLoS ONE. 2012; 7:e23046.

11. Haka AS, Shafer-Peltier KE, Fitzmaurice M, Crowe J, Dasari RR, Feld MS. Proc Natl Acad Sci. 2005; 102:12371–12376. [PubMed: 16116095]
12. Kang JW, Lue N, Kong CR, Barman I, Dingari NC, Goldfless SJ, Niles JC, Dasari RR, Feld MS. Biomed Opt Express. 2011; 2:2484–2492. [PubMed: 21991542]
13. Saha A, Barman I, Dingari NC, McGee S, Volynskaya Z, Galindo LH, Liu W, Plecha D, Klein N, Dasari RR, Fitzmaurice M. Biomed Opt Express. 2011; 2:2792–2803. [PubMed: 22025985]
14. Wood BR, McNaughton D. J Raman Spectrosc. 2002; 33:517–523.
15. Manoharan R, Wang Y, Feld MS. Spectrochim Acta A. 1996; 52A:215–249.
16. Harz M, Kiehntopf M, Stockel S, Rösch P, Staube E, Deufel T, Popp J. J Biophotonics. 2009; 2:70–80. [PubMed: 19343686]
17. Maquelin K, Kirschner C, Choo-Smith LP, Ngo-Thi NA, Van Vreeswijk T, Stammler M, Endtz HP, Bruining HA, Naumann D, Puppels GJ. J Clin Microbiol. 2003; 41:324–329. [PubMed: 12517868]
18. Somorjai RL, Dolenko B, Baumgartner R. Bioinformatics. 2003; 19:1484–1491. [PubMed: 12912828]
19. Buijtels PCAM, Willemse-Erix HFM, Petit PLC, Endtz HP, Puppels GJ, Verbrugh HA, Belkum AV, Soolingen DV, Maquelin K. J Clin Microbiol. 2008; 46:961–965. [PubMed: 18174303]
20. Fitzmaurice M. J Biomed Opt. 2000; 5:119–130. [PubMed: 10938775]
21. Kingma KJ, Hemly RJ. Am Mineral. 1994; 79:269–273.
22. McMillan F, Wolf GH, Lambert P. Phys Chem Miner. 1992; 19:71–79.
23. Handbook of Raman Spectra (free database 2000–2002 Laboratoire des Sciences de la Terre ENS-Lyon France).
24. Alison AC, Hart DA. Br J Exp Pathol. 1968; 49:465–476. [PubMed: 4302496]
25. Heppieston AG. Med Bull. 1969; 25:282.
26. Das S, Mandal S, Chakraborty AN, Dastidar SG. Ind J Med Res. 1992; 95:59–65.
27. Guerra, EG. Encyclopaedia of occupational health and safety. Vol. II. International Labour Office; Geneva: 1974.
28. Shen FZ. Chin J Tuberc Respir Dis. 1991; 14:292–320.
29. Chatterjee A, Das S. J Biomed Pharm Sciences. 2011; 1:8–12.
30. Das S, Chattopadhyay UK. Indian J Tuberc. 2000; 47:87–92.
31. Thomas Oleary F. Chest. 1939; 5:18–20.
32. Higgins DA, Kung IT, Or RS. Infect Immun. 1985; 48:252–256. [PubMed: 2984123]
33. Ullas G, Nayak SS, Gopalkrishna K, Jacob J, Kurein J, Pai KM, Vengul M, Valiathan M, Lakshmi RJ, Krishna KV, Raghavendra K, Kartha VB. Curr Sci. 1999; 77:908–914.
34. Ashwin Kumar M, Sreedhar S, Barman I, Dingari NC, Venugopal Rao S, Prem Kiran P, Tewari SP, Manoj Kumar G. Talanta. 2011; 87:53–59. [PubMed: 22099648]
35. Dingari NC, Barman I, Ashwin Kumar M, Tewari SP, Manoj Kumar G. Anal Chem. 2012; 84:2686–2694. [PubMed: 22292496]

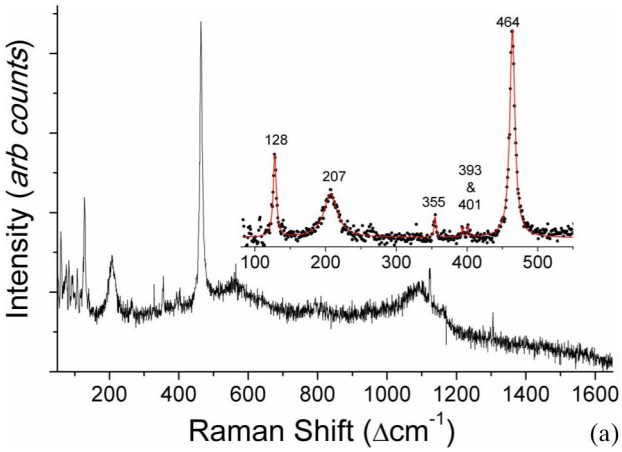

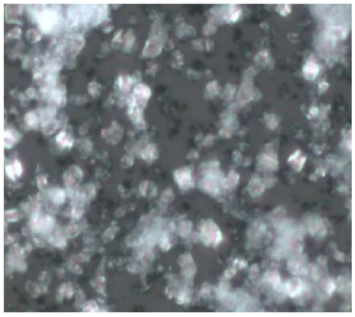

Figure 1.

(online color at: www.biophotonics-journal.org) (**a**) Typical Raman spectra of the CSF sample clinically diagnosed as tuberculosis meningitis and (**b**) its microscopic image (50X objective), which shows crystalline structures.

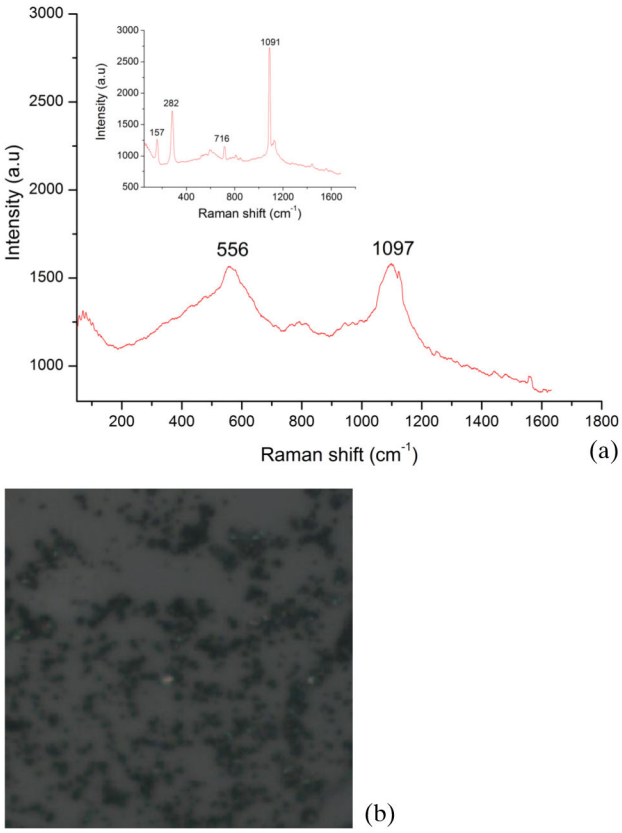

Figure 2.

(online color at: www.biophotonics-journal.org) (**a**) and its inset show the typical Raman spectra of two CSF samples clinically diagnosed as non-meningitis and (**b**) the microscopic image (50X objective), of the CSF sample in (**a**), which does not show crystalline structures as in the case of the TBM CSF sample in Figure 1(b).

Table 1

Raman peaks with their symmetry modes.

Wave number (cm^{-1})	Raman Band Assignment	Mode of Symmetry
128	Silicates (*α*-quartz phase)	$E_{ILO+TOJ}$
157	Calcite	–
207	Silicates (*α*-quartz phase)	A1 (non– degenerate symmetric stretch)
282	Carbonates	–
355, 393, 401	Silicates	–
464	Silicates (*α*-quartz phase)	A1 (non– degenerate symmetric stretch)
556	Carbonates	–
716	Calcite	V4 (symmetric bend)
1091, 1094	Calcite	V1 (symmetric stretching bend)
1124	Carbonates	–